LINEAR STABILITY ANALYSIS OF GRAVITATIONAL EEFFECTS ON A LOW-DENSITY GAS JET INJECTED INTO A HIGH-DENSITY MEDIUM

Anthony L. Lawson and Ramkumar N. Parthasarathy

School of Aerospace and Mechanical Engineering

The University of Oklahoma

Norman, Oklahoma 73019

rparthasarathy@ou.edu

ABSTRACT

The objective of this study was to determine the effects of buoyancy on the absolute instability of low-density gas jets injected into high-density gas mediums. Most of the existing analyses of low-density gas jets injected into a high-density ambient have been carried out neglecting effects of gravity. In order to investigate the influence of gravity on the near-injector development of the flow, a spatio-temporal stability analysis of a low-density round jet injected into a high-density ambient gas was performed. The flow was assumed to be isothermal and locally parallel; viscous and diffusive effects were ignored. The variables were represented as the sum of the mean value and a normal-mode small disturbance. An ordinary differential equation governing the amplitude of the pressure disturbance was derived. The velocity and density profiles in the shear layer, and the Froude number (signifying the effects of gravity) were the three important parameters in this equation. Together with the boundary conditions, an eigenvalue problem was formulated. Assuming that the velocity and density profiles in the shear layer to be represented by hyperbolic tangent functions, the eigenvalue problem was solved for various values of Froude number. The Briggs-Bers criterion was combined with the spatio-temporal stability analysis to determine the nature of the absolute instability of the jet – whether absolutely or convectively unstable. The roles of the density ratio, Froude number, Schmidt number, and the lateral shift between the density and velocity profiles on the absolute instability of the jet were determined. Comparisons of the results with previous experimental studies show good agreement when the effects of these variables are combined together. Thus, the combination of these variables determines how absolutely unstable the jet will be.

NOMENCLATURE

English Symbols

C_1 constant of integration of equation (15)

C_2 constant of integration of equation (16)

d nozzle diameter in Cetegen (1997-2)

D jet diameter

D_b binary diffusivity coefficient

Fr Froude number; $Fr^2 = \dfrac{U_j^2}{gR}\dfrac{\rho_j}{\left(\rho_\infty - \rho_j\right)}$

g acceleration due to gravity

G non-dimensional coefficient of the buoyancy term in the pressure disturbance equation; $G = \dfrac{1}{Fr^2 \dfrac{R}{\theta}\left(\dfrac{\rho_\infty}{\rho_j} - 1\right)}$

i $\sqrt{-1}$

k wavenumber

Δk step-size of the real and imaginary parts of the wavenumber

m azimuthal wavenumber

N parameter that controlled the jet mixing layer thickness in Monkewitz and Sohn (1988)

P Prandtl number

p pressure

r radial coordinate

r_o low-density jet exit radius

Δr lateral shift between the inflexion points of velocity and density profiles

R radius of the jet shear layer

R_e radius of the jet exit

Ri Richardson number; $Ri = \frac{gD}{U_j^2}\frac{\left(\rho_\infty - \rho_j\right)}{\rho_j}$

Ri_1 Richardson number; $Ri_1 = \frac{\rho_j}{\rho_\infty} Ri$

S Density ratio

Sc Schmidt number; $Sc = \frac{\upsilon}{D_b}$

t time

T temperature

u jet axial velocity component

U jet base velocity

U_c jet base centerline velocity

v jet radial velocity component

w jet azimuthal velocity component

x axial coordinate

Y_j local mass fraction of injected gas

Greek Symbols

δ_{ij} Kronecker delta

∇ del operator

ϕ azimuthal coordinate

λ wavelength

Λ velocity ratio in Monkewitz and Sohn (1988); $\Lambda = \dfrac{U_j - U_\infty}{U_j + U_\infty}$

μ fluid viscosity

υ fluid kinematic viscosity

ρ fluid mass density

ρ_j fluid mass density of low-density gas

ρ_∞ fluid mass density of high-density ambient gas

θ shear layer momentum thickness

Ω angular frequency

Superscripts

( )' fluctuations

($\bar{}$) averaged variable

($\hat{}$) amplitude of variable

($\tilde{}$) dimensional variable

Subscripts

∞ ambient gas property

j low-density gas property

1. Introduction

Plumes of diffusion flames, fuel leaks, engine and industry exhaust, propulsion in space, materials processing, and natural phenomena such as fires and volcanic eruptions are a few examples of low-density gas jets injected into higher density ambient gases encountered in many engineering and technical applications. A number of experimental studies[1-4] indicate that at certain conditions, low-density gas jets injected into high-density gases may sustain an absolute instability leading to highly periodic oscillations. A similar phenomenon is observed in the flickering of diffusion flames that is attributed to buoyancy[5,6]. Recent experimental studies in drop-towers[7,8] also indicate that the observed periodic oscillations vanish when effects of gravity are removed. This served as the motivation for the present investigation to study the influence of gravity on the disturbances in the near-injector region of low-density jets. This study aims to highlight and improve our understanding of the nature of flow instability in low-density round gas jets injected into high-density gases.

Round jets with homogeneous shear layers have been studied extensively in the past. The near-injector region of a round jet, as influenced by disturbances, has a direct influence on the flow development in the far-field of the jet. Several authors[9-11] have shown that linear stability analysis models the large-scale structures of the near-injector region well. Batchelor and Gill[12] studied the stability of steady unbounded axisymmetric single-phase jet flows of the wake-jet type with nearly parallel streamlines and obtained the critical Reynolds number of the jet. Mollo-Christensen[13] and Crow and Champagne[14] found that the near-injector large-scale structure of jet turbulence was well

modeled by linear stability theory. Gaster et al.[15] applied the inviscid stability theory to model the large-scale vortex structures that occurred in a forced mixing layer. The comparison between experimental data and computational models showed that the agreement in both amplitude and phase velocity of the disturbances across the various sections of the flow was excellent on a purely local basis. Michalke[16] reviewed early studies of jet instability. These studies were carried out to understand the transition from laminar flow to turbulence and to describe the evolution of the large-scale coherent structures in the near-injector field. The analysis was based on the locally parallel flow assumption and the neglect of fluid viscosity, heat conduction and dissipation, and gravitational effects. Small disturbances in the form of normal modes were introduced in the equations of motion and the equations were linearized. The critical Reynolds number denoting the transition from laminar to turbulent flow was found. Also, the streak line patterns obtained using the results of the linear stability analysis were in good agreement with the first-stage of the vortex rolling-up process that was observed experimentally in the near-injector field. Cohen and Wygnanski[17] concluded that the linear stability analysis was able to correctly predict the local distribution of amplitudes and phases in an axisymmetric jet that was excited by external means. The analysis was also capable of predicting the entire spectral distribution of velocity perturbations in an unexcited jet over a short distance in the streamwise direction.

Monkewitz and Sohn[18] re-examined the linear inviscid stability analysis of compressible heated axisymmetric jets with particular attention to the impulse response of the flow. Two different responses were identified based on the results. In one case, the flow was absolutely unstable, when a locally generated small disturbance grew

exponentially at the site of the disturbance and eventually affected the entire flow region. In the other case termed convective instability, the disturbance was convected downstream leaving the mean flow undisturbed. It was shown that heated (low-density) jets injected into ambient gas of high density developed an absolute instability and became self-excited when the jet density was less than 0.72 times the ambient gas density. The critical density ratio (demarcating absolute and convective stability) was much lower, about 0.35, for the first azimuthal wavenumber mode than that for the axisymmetric wavenumber mode. This indicated the dominance of the axisymmetric mode during jet instability for high-density ratios. Yu and Monkewitz[19] carried out a similar analysis for two-dimensional inertial jets and wakes with non-uniform density and axial velocity profiles. Again, gravitational effects were neglected and the flow was assumed to be locally parallel. It was found that the absolute frequencies and wavenumbers of small disturbances in the near-injector region scaled with the jet/wake width and not on the thickness of the individual mixing layers, suggesting that the absolute instability was brought about by the interaction of the two mixing layers. Jendoubi and Strykowski[20] considered the stability of axisymmetric jets with external co-flow and counterflow using linear stability analysis. The boundaries between absolute and convective instability were distinguished for various parameters: jet-to-ambient velocity ratio, density ratio, jet Mach number, and the shear layer thickness in the absence of gravitational effects. Raynal et al.[21] carried out experiments with variable-density plane jets issuing into ambient air. A range of density ratios (0.14 to 1) and a range of Reynolds numbers based on the slot width and the jet fluid viscosity (250 to 3000) were studied. It was found that when the jet to ambient fluid density ratio was less

than 0.7, the jets exhibited self-excited oscillations. Theoretical results based on the analysis of Yu and Monkewitz[19] indicated the presence of absolute instability for density ratios less than 0.94 for plane jets, which was different from the value of 0.7 observed in experiments. Raynal et al.[21] attempted to explain this discrepancy by taking into account the differences in the location of the inflection points in the density and velocity profiles for the cases of heated jets injected into air and the isothermal helium-air jets injected into air.

Note that gravitational effects have been neglected in all of the analyses listed above. The neglect of gravitational effects has been justified by the authors because of the small magnitude of the Richardson number based on the jet velocity and jet diameter. However, within the shear layer where the density and velocity change from jet to ambient values, the gravitational effects may not be negligible. The present study extends the work of Michalke and Hermann[22]to consider the effects of gravity on the instability of a low-density gas injected into a high-density ambient. The specific objectives of the study were:

(a) to determine the effects of buoyancy on the absolute stability of low-density round jets injected into high-density ambient gases by performing a linear spatio-temporal stability analysis; and

(b) to determine the nature of the instabilities, whether absolute or convective, and to demarcate the boundary separating the two modes of instability.

2. Theory

A round low-density gas jet (radius R and density ρ_j) is discharged into a high-density ambient gas medium (density ρ_∞) at atmospheric pressure. The basic jet flow is assumed to be a locally inviscid parallel flow with an axial velocity component varying radially. The flow is assumed to be isothermal to simplify the analysis. The radial velocity of the jet is considered small and, therefore, neglected. This corresponds to the "locally-parallel" assumption normally used in the linear stability analysis.

Representing the velocity components by $(\tilde{u},\tilde{v},\tilde{w})$, in cylindrical coordinates $(\tilde{x},\tilde{r},\phi)$ centered at the origin of the jet, the conservation equations governing the flow are :

$$\frac{\partial\tilde{\rho}}{\partial t}+\frac{\partial(\tilde{\rho}\tilde{u})}{\partial\tilde{x}}+\frac{1}{\tilde{r}}\frac{\partial(\tilde{r}\tilde{\rho}\tilde{v})}{\partial\tilde{r}}+\frac{1}{\tilde{r}}\frac{\partial(\tilde{\rho}\tilde{w})}{\partial\phi}=0 \qquad (1)$$

$$\tilde{\rho}\left[\frac{\partial\vec{v}}{\partial t}+\vec{v}\bullet\nabla\vec{v}\right]=-\nabla p+g(\rho_\infty-\tilde{\rho})\delta_{i1}+\nabla\bullet(\mu\nabla\vec{u}) \qquad (2)$$

where g is the acceleration due to gravity and δ_{i1} is the Kronecker delta function with i = 1 representing the axial direction. The binary mass diffusion equation for the diffusion of the injected gas in the ambient gas medium is given in terms of the local mass fraction of the injected gas[23]:

$$\tilde{\rho}\left[\frac{\partial Y_j}{\partial t}+\vec{v}\bullet\nabla Y_j\right]=\nabla\bullet\left[\tilde{\rho}D_b\nabla Y_j\right] \qquad (3$$

In the linear stability analysis, the variables are represented as the sum of the base state value and a fluctuation. Substitution of these variables into equations (1) and (2), linearization, and the neglect of viscous and diffusive terms, yields

$$\frac{\partial \rho'}{\partial t}+\bar{u}\frac{\partial \rho'}{\partial \tilde{x}}+\bar{\rho}\frac{\partial u'}{\partial \tilde{x}}+\frac{1}{\tilde{r}}\frac{\partial\left(\tilde{r}\bar{\rho}v'\right)}{\partial \tilde{r}}+\frac{\bar{\rho}}{\tilde{r}}\frac{\partial w'}{\partial \phi}=0 \tag{5}$$

$$\bar{\rho}\left[\frac{\partial u'}{\partial t}+\bar{u}\frac{\partial u'}{\partial \tilde{x}}+v'\frac{d\bar{u}}{d\tilde{r}}\right]=-\frac{\partial p'}{\partial \tilde{x}}-g\rho' \tag{6}$$

$$\bar{\rho}\left[\frac{\partial v'}{\partial t}+\bar{u}\frac{\partial v'}{\partial \tilde{x}}\right]=-\frac{\partial p'}{\partial \tilde{r}} \tag{7}$$

$$\bar{\rho}\left[\frac{\partial w'}{\partial t}+\bar{u}\frac{\partial w'}{\partial \tilde{x}}\right]=-\frac{1}{\tilde{r}}\frac{\partial p'}{\partial \phi} \tag{8}$$

The density of the mixture is related to the mass fraction by

$$\tilde{\rho}=\frac{\rho_j}{Y_j+\left(1-Y_j\right)S} \tag{9}$$

Substituting for Y_j in equation (3), linearizing and neglecting the diffusive term, we obtain

$$\frac{\partial \rho'}{\partial t}+\bar{u}\frac{\partial \rho'}{\partial \tilde{x}}+v'\frac{d\bar{\rho}}{d\tilde{r}}=0 \tag{10}$$

Using equation (10), equation (5) reduces to

$$\bar{\rho}\left[\frac{\partial u'}{\partial \tilde{x}}+\frac{1}{\tilde{r}}\frac{\partial\left(\tilde{r}v'\right)}{\partial \tilde{x}}+\frac{1}{\tilde{r}}\frac{dw'}{d\phi}\right]=0 \tag{11}$$

The fluctuations are assumed to be normal mode disturbances given by

$$\left(u',v',w',p',\rho'\right)=\left[\hat{u}\left(\tilde{r}\right),\hat{v}\left(\tilde{r}\right),\hat{w}\left(\tilde{r}\right),\hat{p}\left(\tilde{r}\right),\hat{\rho}\left(\tilde{r}\right)\right]e^{i\left(\tilde{k}\tilde{x}-\tilde{\Omega}t+m\phi\right)} \tag{12}$$

Substituting the expressions (12) in equations (6), (7), (8), (9) and (10), we obtain the pressure disturbance equation:

$$\frac{d^2\hat{p}}{d\tilde{r}^2}+\left[\frac{1}{\tilde{r}}-\frac{2\dfrac{d\bar{u}}{d\tilde{r}}}{\bar{u}-\dfrac{\tilde{\Omega}}{\tilde{k}}}-\frac{1}{\bar{\rho}}\frac{d\bar{\rho}}{d\tilde{r}}\left(1+\frac{ig}{\tilde{k}\left(\bar{u}-\dfrac{\tilde{\Omega}}{\tilde{k}}\right)^2}\right)\right]\frac{d\hat{p}}{d\tilde{r}}-\left(\tilde{k}^2+\frac{m^2}{\tilde{r}^2}\right)\hat{p}=0 \quad (13)$$

Nondimensionalizing equation (12) using ρ_∞, U_j, and θ (the momentum thickness of the jet boundary layer); and setting m = 0 gives the nondimensionalized pressure disturbance equation - for the varicose mode:

$$\frac{d^2P}{dr^2}+\left[\frac{1}{r}-\frac{2\dfrac{dU}{dr}}{U-\dfrac{\Omega}{k}}-\frac{1}{\rho}\frac{d\rho}{dr}\left(1+i\frac{1}{Fr^2\dfrac{R}{\theta}\left(\dfrac{\rho_\infty}{\rho_j}-1\right)k\left(U-\dfrac{\Omega}{k}\right)^2}\right)\right]\frac{dP}{dr}-k^2P=0 \quad (14)$$

With no density gradient equation (14) reduces to the equation governing the instability of constant-density jets[22]. Also, as $r\to\infty$, and if gravitational effects are neglected, equation (14) is identical to the equation used by Yu and Monkewitz[19] and Raynal et al.[21] in the analysis of plane jets. Inclusion of buoyancy effects indicates that the stability characteristics are altered by the additional term present in equation (14). Thus, an eigenvalue problem is posed, for specified mean velocity and density profiles, by equation (14) along with the boundary conditions:

$$\begin{aligned} &P(\infty)\to 0 \\ &P(0) \text{ is finite} \\ &\frac{dP(0)}{dr}=0 \quad \text{due to symmetry} \end{aligned} \qquad (15)$$

As $r\to 0$ and $r\to\infty$, $\dfrac{dU}{dr}$ and $\dfrac{d\rho}{dr}$ equal zero and the pressure disturbance equation (13) reduces to the modified Bessel equation. The solutions of the modified Bessel equation satisfying the boundary conditions (14), as $r\to 0$ and $r\to\infty$, are

$$P^{(i)} = C_1 I_m\left(kr\right) \qquad P^{(o)} = C_2 K_m\left(kr\right) \tag{16}$$

respectively, where the superscripts *i* and *o* represent the inner and outer solutions respectively. I_m and K_m are the modified Bessel functions of the order m and C_1 and C_2 are arbitrary constants.

The basic jet velocity profile, $\bar{u}(r)$, is given by that used by Michalke and Hermann[22],

$$\frac{\bar{u}(\tilde{r})-U_\infty}{U_j-U_\infty} = 0.5\left\{1-\tanh\left[0.25\frac{R}{\theta}\left(\frac{\tilde{r}}{R}-\frac{R}{\tilde{r}}\right)\right]\right\} \tag{17}$$

where U_j is the injected jet uniform velocity and U_∞ is the uniform co-flow velocity. For this study the co-flow velocity was set to zero for a quiescent ambient gas and *R* is the radius of the jet defined as the radial location corresponding to the center of the shear layer. As shown by Crighton and Gaster[24],

$$\frac{R}{\theta} = \frac{100}{3\frac{\tilde{x}}{R}+4} \tag{18}$$

for no co-flow. The values of the jet parameter used in this study are 25, 10 and 5 corresponding to $\tilde{x}/(2R)$ = 0, 1 and 2.67. This is within the near-injector region of the jet and allows for the effects of buoyancy to manifest as the jet proceeds downstream. Figure 1 illustrates the basic jet velocity profiles at these three locations. The shear layer widens as the jet proceeds downstream from R/θ = 25 to R/θ = 5 indicating the downstream development of the jet. A hyperbolic tangent profile is also assumed for the basic density profile in the shear layer,

$$\frac{\bar{\rho}(r)}{\rho_\infty} = 1+\left(\frac{\rho_j}{\rho_\infty}-1\right)\left\{0.5\left(1-\tanh\left[0.25\frac{R}{\theta}\left(\frac{\tilde{r}}{R}-\frac{R}{\tilde{r}}\right)\right]\right)\right\} \tag{19}$$

Figure 2 illustrates the density profiles at R/θ = 10 for ρ_j/ρ_∞ = 1, 0.6, and 0.14.

The effects of buoyancy on the jet were studied by investigating the variation of the real and imaginary parts of both the complex wavenumber and frequency with the Froude number. The Froude number is the ratio of the inertia force to buoyancy force and is defined as

$$Fr^2 = \frac{U_j^2}{gR}\frac{\rho_j}{\rho_\infty - \rho_j} \tag{20}$$

To solve the disturbance equation (14), a fourth-order Runge-Kutta scheme with automatic step-size control is used to integrate the equation (14). The infinite integration domain, $0 < r < \infty$ is divided into two finite domains: an inner domain $R \geq r \geq 0$ and an outer domain $r_\infty \geq r \geq R$, where R is the jet radius and r_∞ is a specified large radius where the gradients of the velocity and density are small. A shooting method is used to determine $\Omega(k)$ such that both P and $\frac{dP}{dr}$ are continuous at $r = R$. A parabolic complex zero-search procedure was used to vary Ω for a specified k until the matching conditions were satisfied to a minimum accuracy within 10^{-10}.

For the spatio-temporal linear stability analysis, both the frequency and wavenumber are considered complex. The spatio-temporal linear stability along with the Briggs-Bers criterion[25, 26] was used to determine the absolute stability and the nature of the absolute stability of the jet. The jet is said to be absolutely unstable when the complex frequency eigenvalue is a saddle point and its imaginary part is greater than zero. If its imaginary part is less than zero, the jet is convectively unstable. Therefore, the saddle points in the complex (Ω, k) domain were determined and the satisfaction of the pinching requirements was verified using the mesh-searching technique described by Li and

Shen[27].

3. Results and Discussion

Preliminary calculations confirmed the conclusion of Monkewitz and Sohn[18] that the varicose mode (m = 0) is more absolutely unstable than the sinuous mode (m = 1) in the near-injector region of round jets. This is illustrated in Figure 3. Figure 3 depicts the variation of the absolute temporal growth rate Ω_i^o with density ratio of an inviscid top-hat jet bounded by a cylindrical vortex sheet at m = 0 and m = 1. At all density ratios studied, Ω_i^o values are higher for the varicose mode than for the sinuous mode. Also, the density ratio at which Ω_i^o first becomes positive, as density ratio is reduced, is higher for the varicose mode (at a density ratio of 0.66) than for the sinuous mode (at a density ratio of 0.35). Therefore, the following results on the instability of a low-density round gas jet injected into a high-density ambient gas concentrate on the varicose mode (m = 0).

Results of the temporal stability analysis of low-density jets injected into a high-density ambient gas were first carried out[28]. A non-dimensional parameter, G, was found to play an important role in the temporal instability:

$$G = \frac{1}{Fr^2 \frac{R}{\theta}\left(\frac{\rho_\infty}{\rho_j} - 1\right)} \qquad (21)$$

G is a non-dimensional number that compares the acceleration of the large-scale structures of the jet due to buoyancy to that due to inertial forces. It was found that the effect of buoyancy at low Fr values was to cause the jet instabilities to increase exponentially.

The focus of this paper is the effects of the inhomogeneous shear-layer and buoyancy on the nature of the absolute instability. This was done by first studying the effect of varying the density ratio from 0.99 to 0.14, while varying the Froude number from infinity to 0.5. The complex frequency Ω and the complex wavenumber k are normalized in the present results using the shear-layer momentum thickness θ and the velocity difference $\Delta U = U_j - U_\infty$. First, the present results were compared with those of Monkewitz and Sohn[19] and a favorable agreement was obtained[28].

Effect of density ratio

The imaginary part Ω_i^o of the complex absolute frequency, in this study, denotes the absolute temporal growth rate of the disturbances. When Ω_i^o is positive (and the Briggs-Bers criterion is satisfied) the jet is absolutely unstable while for a negative Ω_i^o the jet may be convectively unstable. A constant-density jet (such as an air-in-air jet) is convectively unstable; as the density ratio is reduced (a low-density jet injected into a high-density gas medium), the nature of instability of the jet is changed from convective instability to absolute instability. This density ratio, at which the jet first becomes absolutely unstable, is referred to as the critical density ratio (S_c). In Figure 3, for example, this is the density ratio at which $\Omega_i^o = 0$. The real part Ω_r^o of the absolute complex frequency is the frequency corresponding to the absolute temporal growth rate of the disturbance. The imaginary part k_i^o of the complex wavenumber is the absolute spatial growth rate of the disturbances. Figure 4 depicts the variation of the absolute temporal growth rate of the disturbances with the density ratio at $R/\theta = 10$ and 5 with Froude number fixed at infinity (no buoyancy effects). At $R/\theta = 10$, the growth rate is increased by about 201%, as the density ratio is reduced from 0.99 to 0.14 . The critical

density ratio, S_c, at this location is 0.525. The absolute growth rates of the jet disturbance are positive for density ratios below 0.525 indicating that the jet is absolutely unstable. However, for density ratios above 0.525 the absolute growth rates are negative meaning the jet is convectively unstable.

As the jet proceeds downstream from an axial location corresponding to $R/\theta = 10$ to $R/\theta = 5$, the absolute temporal growth rates decrease for all density ratios. The absolute temporal growth rates are decreased by about 76% at a density ratio of 0.14 and by about 316% at a density ratio of 0.99 (the other extreme of the range of density ratios studied). The percentage decrease in the growth rates for density ratios between 0.14 and 0.99 is increased from 76% to 316%. Trends similar to those observed at $R/\theta = 10$ for the growth rates are also observed at $R/\theta = 5$, but the critical density ratio is decreased to 0.17. Figure 4 illustrates the change in critical density ratio as the jet proceeds from $R/\theta = 10$ to $R/\theta = 5$.

The variation of the real part of the absolute frequency Ω_r^o as the density ratio is increased from 0.14 to 0.99 for $R/\theta = 10$ and 5 is illustrated in Figure 5. At $R/\theta = 10$ and 5, Ω_r^o is increased by about 107% and 62%, respectively, as the density ratio increased from 0.14 to 0.99. Ω_r^o is increased as the flow proceeds from $R/\theta = 10$ to 5 at all density ratios. At extremes of the range of density ratios investigated (0.14 and 0.99) Ω_r^o is increased by about 83% and 43%, respectively, as the flow proceeds from $R/\theta = 10$ to 5.

The absolute spatial growth rates $-k_i^o$ are plotted against density ratio for $R/\theta = 10$ and 5 in Figure 6. At $R/\theta = 10$, the absolute spatial growth rate is increased by about 76% as the density ratio is increased from 0.14 to 0.99. At $R/\theta = 5$, the absolute spatial growth

rate is increased by about 71% as the density ratio is increased from 0.14 to 0.99. And, as the jet proceeds downstream from $R/\theta = 10$ to $R/\theta = 5$, the absolute spatial growth rates are increased by about 65% at density ratio = 0.14 and by about 60% at density ratio = 0.99.

Figure 7 illustrates the variation of the real part of the absolute wavenumber k_r^o as the density ratio is increased from 0.14 to 0.99 for R/θ values of 10 and 5. At $R/\theta = 10$, k_r^o is increased by about 47% as the density ratio is increased from 0.14 to 0.99 while at $R/\theta = 5$, k_r^o is increased by about 27% as the density ratio is increased from 0.14 to 0.99. And, as the jet proceeds from $R/\theta = 10$ to $R/\theta = 5$, k_r^o is increased by about 70% and 47% at density ratios of 0.14 and 0.99 respectively.

The above trends of the real and imaginary parts of the saddle points (Ω^o, k^o) are similar to those presented by Monkewitz and Sohn[19] in their study on the absolute instability of hot jets at an axial location of $x/R = 2$ ($R/\theta = 10$), with buoyancy effects neglected. Next, buoyancy effects are introduced and the influence of buoyancy on the jet instability is discussed.

Effect of buoyancy

Figures 8 and 9 illustrate the variation of the absolute temporal growth rate of the disturbances with the density ratio for several Froude numbers at $R/\theta = 10$ and 5 respectively. At both $R/\theta = 10$ and 5, as the Froude number is reduced from infinity the absolute temporal growth rate varies with the density ratio only, but below a Froude number of 2 the absolute temporal growth rate varies with both the density ratio and Froude number. For $R/\theta = 10$, the absolute temporal growth rate is increased as the

density ratio is reduced for large Froude numbers. As the density ratio is reduced from 0.14 to 0.99, the absolute temporal growth rate is increased by about 200% at Fr = ∞ and 10. At Fr = 5, the absolute temporal growth rate is increased by about 188%. For Fr = 2, 1.58, and 1, the absolute temporal growth rates are enhanced by about 131%, 99%, and 20% respectively. Below a Froude number of unity, this trend is reversed.. At Fr = 0.75 and 0.5, the absolute temporal growth rates are increased by about 28% and 76% respectively, as the density ratio is increased from 0.14 to 0.99. The absolute temporal growth rates are higher at each density ratio as the Froude number alone is decreased below Fr = 5. For Fr ≥ 5, there is no significant change in the absolute temporal growth rates due to changes in the Froude number, indicating that the jet is momentum-driven at Fr ≥ 5 and that effects of buoyancy are small. At R/θ = 5, the trend is reversed at Froude numbers below 0.75 and the same trends observed at R/θ = 10 are observed at this downstream location also.

As noted earlier, the critical density ratio below which the jet is absolutely unstable for a given Froude number is of interest. Figures 10 and 11 depict the variation of the critical density ratio with Froude number at R/θ = 10 and 5 respectively. At R/θ = 10, at large Froude numbers, the critical density ratio tends to 0.525, and the “critical Froude number” below which the jet is absolutely unstable for all density ratios studied is 1.58. Thus, at density ratios less than 0.525 the jet is absolutely unstable at this location and for Fr < 1.58 any low-density gas jet injected into a high density ambient gas becomes absolutely unstable at R/θ = 10. For R/θ = 5, as the Froude number tends to a large value, the critical density ratio tends to 0.17 and the “critical Froude number” is

1.015. Thus the critical density ratio and critical Froude number appear to be functions of the shear layer width and thus the axial location downstream of the jet.

The real part of frequencies corresponding to the absolute temporal growth rates of the saddle points discussed above are depicted in Figures 12 and 13 for R/θ = 10 and 5 respectively. Note that the real part of the normalized frequency Ω_r^o might be interpreted as the Strouhal number expressed in terms of the shear-layer momentum thickness, θ and the velocity difference, $\Delta U = U_j - U_\infty$. At R/θ = 10, Ω_r^o is increased by about 105% at Fr ≥ 1.58 as the density ratio is increased from 0.14 to 0.99. Below the critical Fr = 1.58, at this axial location, Ω_r^o is increased by about 102%, 105%, and 112% at Fr = 1, 0.75 and 0.5 respectively as the density ratio is increased from 0.14 to 0.99. Above the critical Fr, Ω_r^o does not change significantly with Fr, although it is a function of density ratio; whereas, below the critical Fr at this location Ω_r^o depends on both the density ratio and Fr, suggesting that the critical Fr demarcates two jet flow regimes. For values less than the critical Fr, the flow is momentum-driven, while at values greater than the critical Fr the flow is within the buoyancy-driven regime. The same trends are noticed at the axial location corresponding to R/θ = 5, and again the dependence on Fr is noticed below the critical Fr, at this location, of 1.015.

From the discussions above it is clear that there is a critical Froude number, which depends on axial location, below which Ω_r^o exhibits a dependence on the Froude number. This is also the Froude number below which the flow is absolutely unstable for all density ratios studied.

Effect of co-flow

Figure 14 illustrates the effect of co-flow on the absolute temporal growth rates of the jet flow at $R/\theta = 10$ for $\rho_j/\rho_\infty = 0.14$ and Fr = ∞, 10, 5, 2, 1, 0.75 and 0.5. Results are presented for co-flow velocity ratios of $U_\infty/\Delta U = 0$, 0.5 (corresponding to $U_\infty = 0.33U_j$), and 1 (corresponding to $U_\infty = 0.5U_j$). As the co-flow is increased ($U_\infty/\Delta U$ is increased from 0 to 1), it is observed that the absolute temporal growth rates of the disturbances decrease linearly at each Fr. An increase in co-flow leads to a decrease in the magnitude of mean shear that serves as the driving force for the instability, thus, resulting in a decrease in the growth rates. As $U_\infty/\Delta U$ is increased from 0 to 1, at this axial location, the absolute growth rates are reduced by about 414% for Fr > 2, and about 359%, 257%, 204%, and 137% at Fr = 2, 1, 0.75 and 0.5 respectively. Though the effect of co-flow is felt less as Fr is decreased, it is obvious from Figure 14 that the presence of co-flow tends to make the previously absolutely unstable flow become convectively unstable. The variation of the real part of the complex absolute frequency Ω_r^o at the saddle points with co-flow is illustrated in Figure 15 for $\rho_j/\rho_\infty = 0.14$ and Fr = ∞, 10, 5, 2, 1, 0.75 and 0.5 at an axial location corresponding to $R/\theta = 10$. An increase in co-flow causes Ω_r^o to increase. As $U_\infty/\Delta U$ is increased from 0 to 1, Ω_r^o is increased by about 53% at all Fr. Note again the reducing effect of co-flow as Fr decreased below 10.

4. Conclusions

In this study, the absolute stability characteristics of a low-density round gas jet injected into a high-density ambient gas were investigated. A linear spatio-temporal stability analysis was performed to solve for eigenvalues of the pressure disturbance equation obtained from the simultaneous solution of the continuity equations and the equations of motion. The equation was solved numerically and a mesh-searching technique was used to determine the saddle points. The limits of the *k*-plane for the mesh-searching technique employed obtained from the results of a linear temporal analysis of a previous paper by the authors. The effects of buoyancy and density ratio on the absolute instability of the jet were investigated using the linear spatio-temporal stability analysis.

Reducing the density ratio steepens the density gradient in the shear layer causing additional disturbance. At a Froude number value of Fr = ∞, as the density ratio reduces, the low-density jet injected into a high-density gas medium becomes absolutely unstable at a critical density ratio of 0.525 and 0.17 at axial locations corresponding to R/θ = 10 and 5 respectively. Below this critical density ratio, reducing the density ratio further causes the jet to become more absolutely unstable. As the Froude number decreases to account for increasing effect of buoyancy, the critical density ratio of the jet increases. Thus, reducing the Froude number has the effect of causing the jet to become absolutely unstable at higher density ratios. At low Froude numbers, buoyancy causes the jet instabilities to increase exponentially which accounts for the abrupt breakdown of the jet large-scale structures observed in experiments at low Froude numbers. There is a critical Froude number below which the jet is absolutely unstable at all density ratios less than

unity. This critical Froude number also demarcates the jet flow into the momentum-driven regime and the buoyancy-driven regime similar to the experimentally-observed Strouhal number regimes. Increasing the co-flow velocity reduces the shear layer thickness and thus the energy available for the growth of the instabilities in the jet. Thus increasing co-flow velocity makes the jet less absolutely unstable. causes the jet to be less absolutely unstable. At lower Froude number values decreasing the relative radial location (negative lateral shift) of the density profile with respect to the velocity profile causes the jet to be more absolutely unstable.

Acknowledgments

This work was supported by a NASA Grant under the Microgravity Fluid Physics Program.

References

[1]Monkewitz, P. A., Bechert, D. W., Barsikow, B. and Lehmann, B. (1990) "Self-excited Oscillations and Mixing in a Heated Round Jet," *Journal of Fluid Mechanics*, Vol. 213, pp. 611-639.

[2]Subbarao, E. R. and Cantwell, B. J., (1992) "Investigation of a Co-Flowing Buoyant Jet: Experiments on the Effects of Reynolds Number and Richardson Number," *Journal of Fluid Mechanics*, Vol. 245, pp. 69-90.

[3]Kyle, D. M. and Sreenivasan, K. R., (1993) "The Instability and Breakdown of a Round Variable-Density Jet," *Journal of Fluid Mechanics*, Vol. 249, pp. 619-664.

[4]Cetegen, B. M. and Kasper, K. D., (1996) “Experiments on the Oscillatory Behavior of Buoyant Plumes of Helium and Helium-Air Mixtures,” *Physics of Fluids*, Vol. 8, No 11, pp. 2974-2984.

[5]Yep, T. W., Agrawal, A. K. and Griffin, D. V. (2003) “Gravitational Effects on Near Field Flow Structure of Low Density Gas Jets,” *AIAA Journal*, Vol. 41, No. 10, pp. 1973-1979.

[6]Pasumarthi, K. (2004) “Buoayncy Effects on Flow Structure and Instability of Low-Density Gas Jets,” *PhD Dissertation*, University of Oklahoma.

[7]Buckmaster, J. and Peters, N., (1986) “The Infinite Candle and its Stability – A Paradigm for Flickering Diffusion Flames,” *Twenty-First Symposium (International) on Combustion*, pp. 1829-1836.

[8]Chen, L. D., Seaba, J. P., Roquemore, W. M., and Goss, L. P. (1988) “Buoyant Diffusion Flames,” *Twenty-Second Symposium (International) on Combustion*, The Combustion Institute, pp. 677-684.

[9]Crow, S. C., (1972) “Acoustic Gain of a Turbulent Jet,” *Paper IE6, Annual Meeting of the Division of Fluid Dynamics of the American Physics Society, Boulder, CO, Nov. 20-22, 1972.*

[10]Moore, C. J., (1977) “The Role of Shear-Layer Instability Waves in Jet Exhaust Noise,” *Journal of Fluid Mechanics*, Vol. 80, Pt. 2, pp. 321-367.

[11]Ffowcs-Williams, J. E. and Kempton, A. J., (1978) “The Noise from the Large-Scale Structure of a Jet,” *Journal of Fluid Mechanics*, Vol. 84, Pt. 4, pp. 673-694.

[12]Batchelor, G. K. and Gill, A. E. (1962) "Analysis of the Stability of Axisymmetric Jets," *Journal of Fluid Mechanics*, Vol. 14, pp. 529-551.

[13]Mollo-Christensen, E. (1967) "Jet Noise and Shear Flow Instability seen from an Experimenter's Viewpoint," Trans. A.S.M.E. E, *Journal of Applied Mechanics*, Vol. 89, pp. 1-7.

[14]Crowe, S. C. and Champagne, F. H. (1971) "Orderly Structure in Jet Turbulence," *Journal of Fluid Mechanics*, Vol. 48, pp. 547-591.

[15]Gaster, M., Kit, E., and Wygnanski, I. (1985) "Large-scale Structures in a Forced Turbulent Mixing Layer," *Journal of Fluid Mechanics*, Vol. 150, pp. 23.

[16]Michalke, A. (1984) "Survey on Jet Instability Theory," *Progress in Aerospace Sciences*, Vol. 21, pp. 159-199.

[17]Cohen, J. and Wygnanski, I. (1987) "The Evolution of the Instabilities in the Axisymmetric Jet. Part 2. The Flow Resulting from the Interaction between Two Waves," *Journal of Fluid Mechanics*, Vol. 176, pp. 221.

[18]Monkewitz, P. A. and Sohn, K. D. (1988) "Absolute Instability in Hot Jets," *AIAA Journal*, Vol. 26, pp. 911-916.

[19]Yu, M.-H. and Monkewitz, P. A. (1990) "The Effect of NonUniform Density on the Absolute Instability of Two-Dimensional Inertial Jets and Wakes," *Physics of Fluids A*, Vol. 2, No. 7, pp. 1175-1181.

[20]Jendoubi, S. and Strykowski, (1994) "Absolute and Convective Instability of Axisymmetric Jets with External Flow," *Physics of Fluids*, Vol. 6, No. 9, pp. 3000-3009.

[21]Raynal, L., Harion, J.-L., Favre-Marinet, M. and Binder, G. (1996) "The Oscillatory Instability of Plane Variable-Density Jets," *Physics of Fluids*, Vol. 8, No. 4, pp. 993-1006.

[22]Michalke, A. and Hermann, G. (1982) “On the Inviscid Instability of a Circular Jet with External Flow,” *Journal of Fluid Mechanics*, Vol. 114, pp. 343-359.

[23]Gebhart, B. (1993) “Heat Conduction and Mass Diffusion,” *McGraw-Hill*, New York.

[24]Crighton, D. G. and Gaster, M. (1976) "Stability of Slowly Diverging Jet Flow" *Journal of Fluid Mechanics*, Vol. 77, pp. 397-413.

[25]Bers, A., (1983) “Space-time Evolution of Plasma Instabilities,” *Handbook of Plasma Physics*, Vol. I, pp. 452-517.

[26]Briggs, R. J., (1964) *Electron Stream Interaction with Plasmas*, MIT Press, Cambridge, Massachusetts.

[27]Li, X. and Shen, J. (1996) “Breakup of Cylinderical Liquid Jets in Co-Flowing Gas Streams,” *ASME*, pp. 22-31.

[28]Lawson, A. L. and Parthasarathy, R. N. (2002) “Linear Temporal Stability Analysis of a Low-Density Round Gas Jet Injected into a High-Density Gas,” *Paper ETCE 2002/CAE-29010, Proceedings of the ASME Engineering Technology Conference on Energy, Houston, TX, Feb. 4-6, 2002.*

[29]Lawson, A. L. (2001) “Instability Analysis of a Low-Density Gas Jet Injected into a High-Density Gas,” *PhD Dissertation*, University of Oklahoma.

LIST OF FIGURES

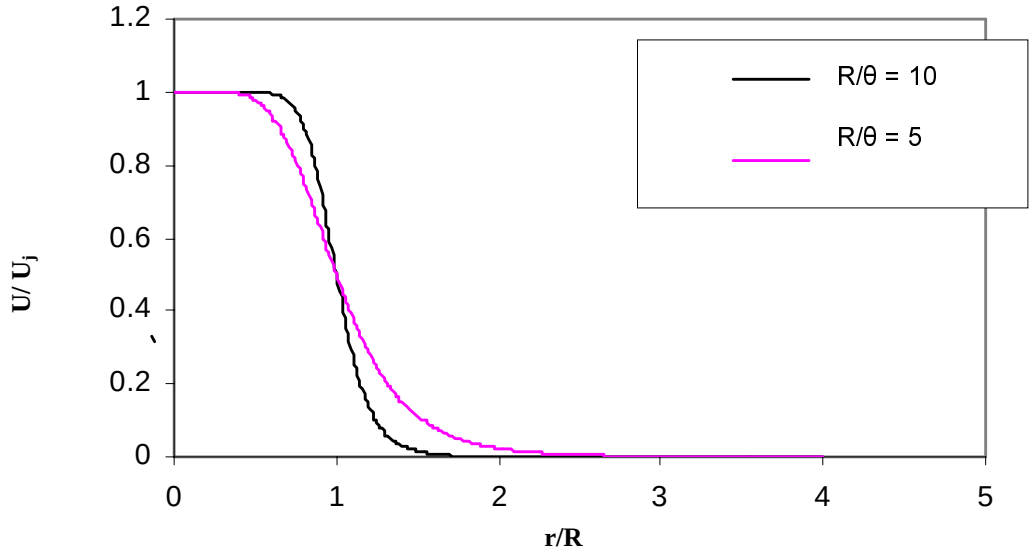
1.2
1
0.8
0.6
0.4
0.2
0
0
1
2
3
4
5
U/ U_j
r/R
R/θ = 10
R/θ = 5

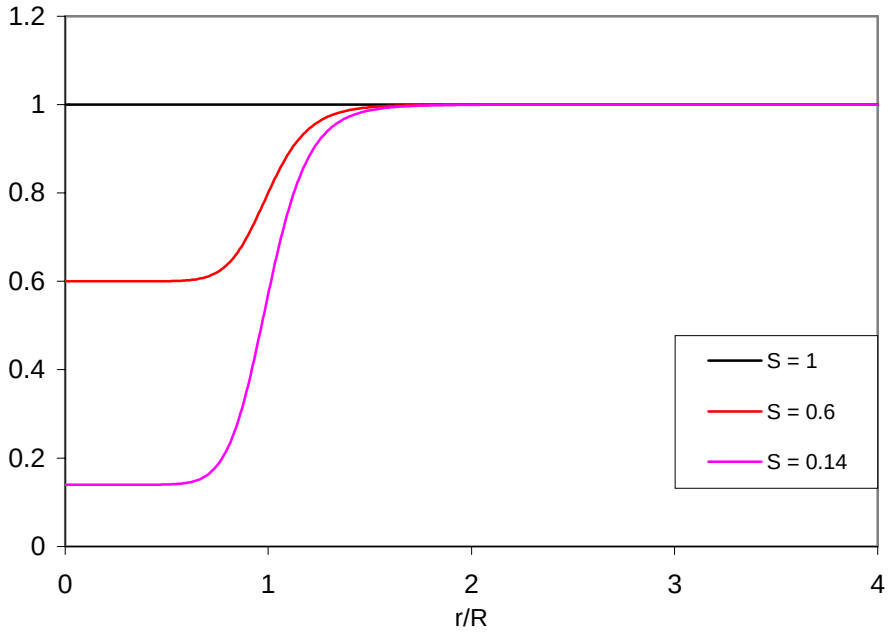
1.2
1
0.8
0.6
0.4
0.2
0
0
1
2
3
4
r/R
S = 1
S = 0.6
S = 0.14

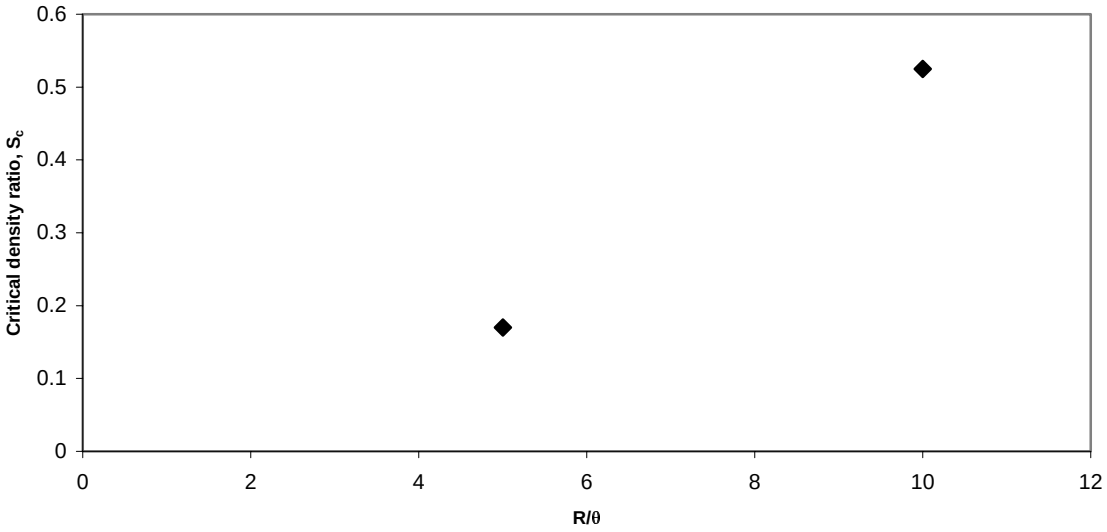
0.6
0.5
0.4
0.3
0.2
0.1
0
Critical density ratio, S_c
0
2
4
6
8
10
12
R/θ

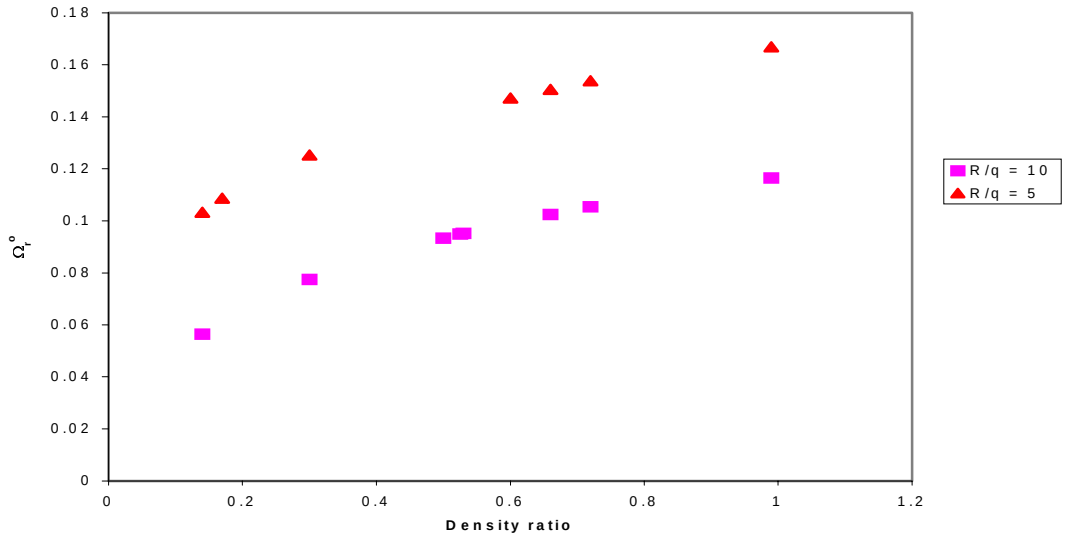
0.18
0.16
0.14
0.12
0.1
0.08
0.06
0.04
0.02
0
Ω_r^o
0
0.2
0.4
0.6
0.8
1
1.2
Density ratio
R/q = 10
R/q = 5

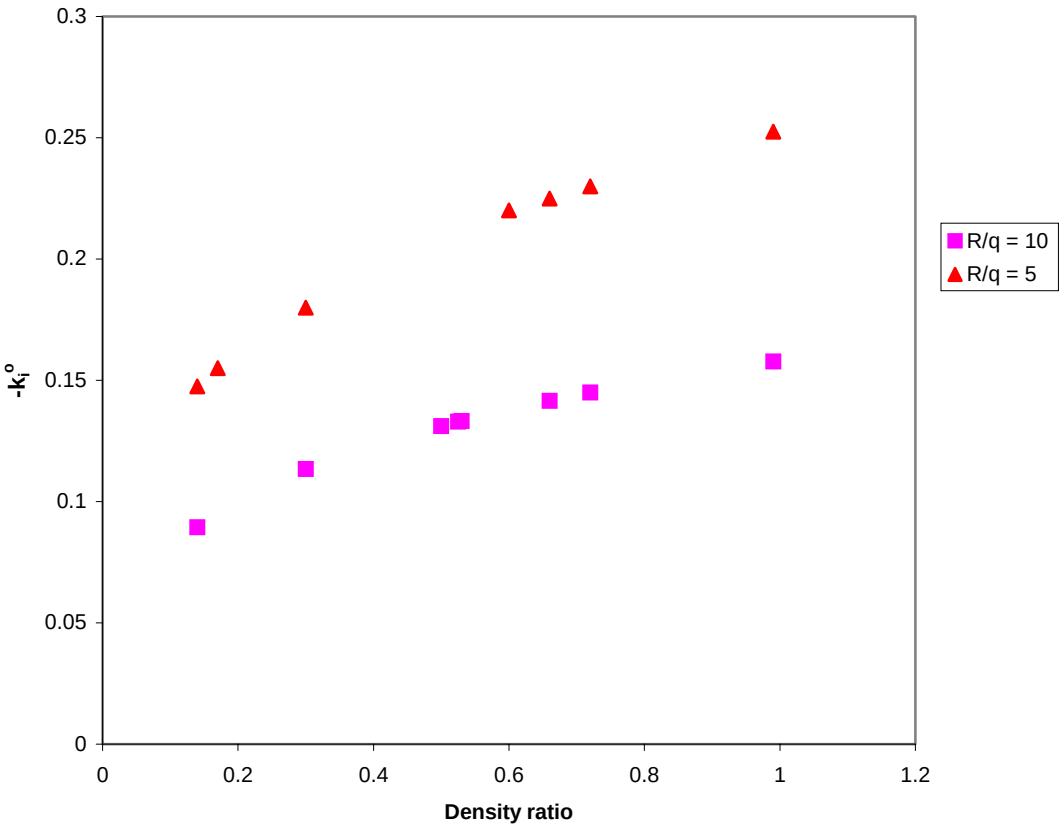
0.3
0.25
0.2
0.15
0.1
0.05
0
-k_i^o
0
0.2
0.4
0.6
0.8
1
1.2
Density ratio
R/q = 10
R/q = 5

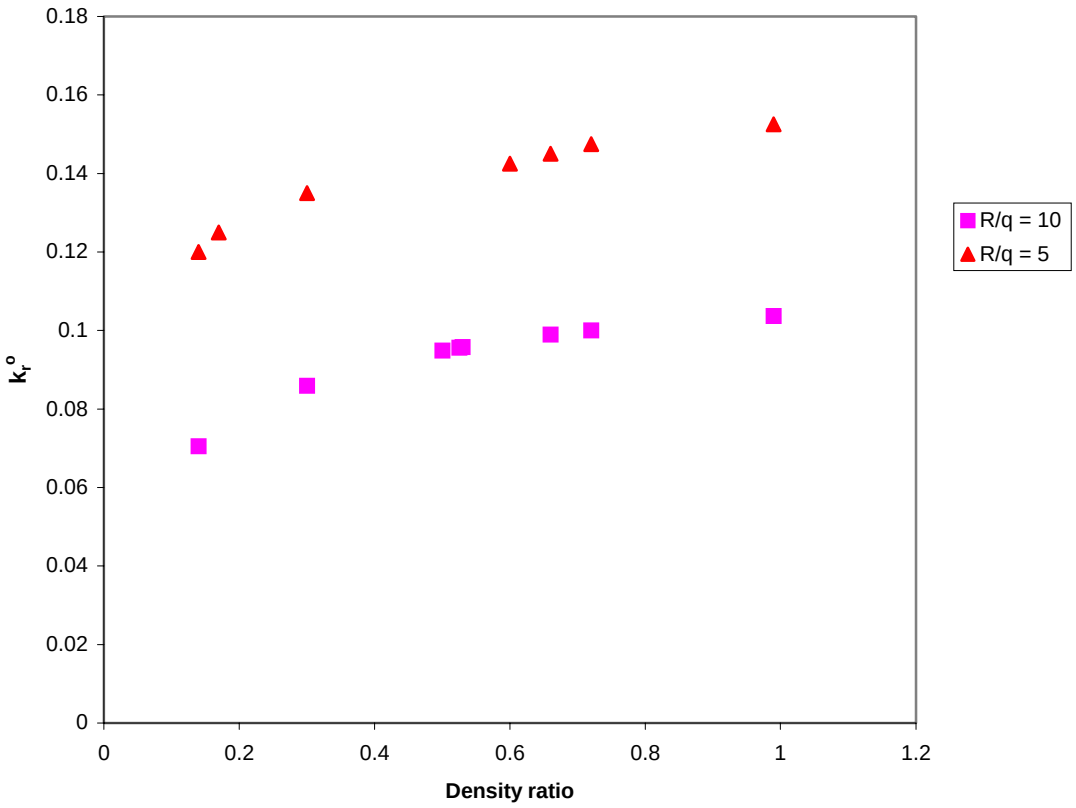
0.18
0.16
0.14
0.12
0.1
0.08
0.06
0.04
0.02
0
k_r^o
0
0.2
0.4
0.6
0.8
1
1.2
Density ratio
R/q = 10
R/q = 5

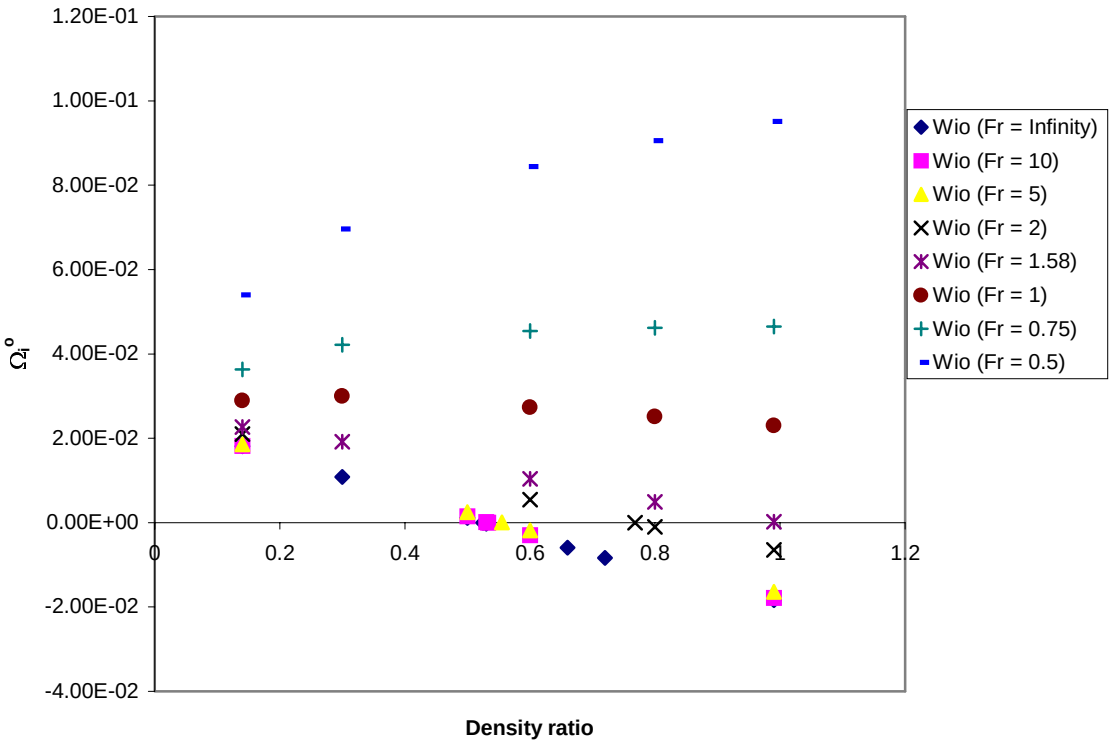
1.20E-01
1.00E-01
8.00E-02
6.00E-02
4.00E-02
2.00E-02
0.00E+00
-2.00E-02
-4.00E-02
Ω_i^o
0
0.2
0.4
0.6
0.8
1
1.2
Density ratio
Wio (Fr = Infinity)
Wio (Fr = 10)
Wio (Fr = 5)
Wio (Fr = 2)
Wio (Fr = 1.58)
Wio (Fr = 1)
Wio (Fr = 0.75)
Wio (Fr = 0.5)

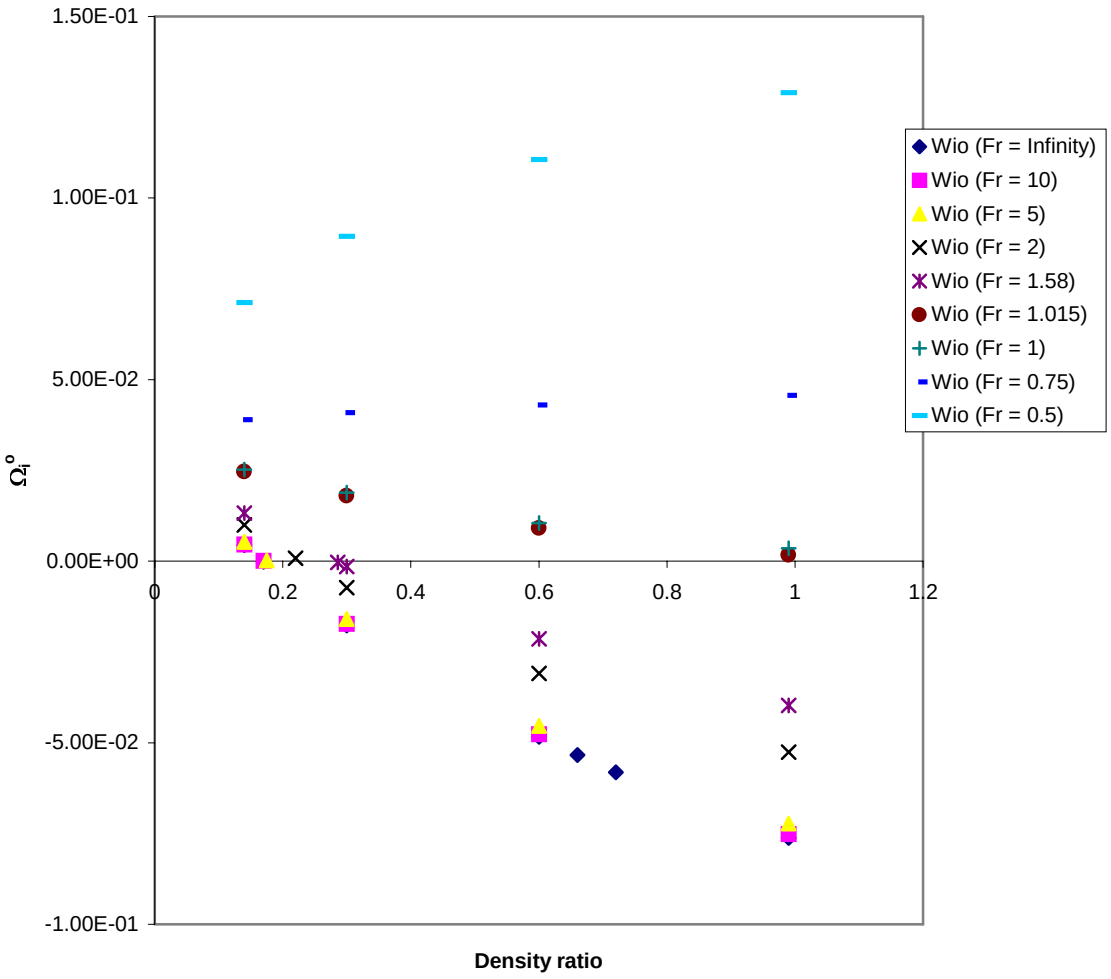
1.50E-01
1.00E-01
5.00E-02
0.00E+00
-5.00E-02
-1.00E-01
0
0.2
0.4
0.6
0.8
1
1.2
Ω_i^o
Density ratio
Wio (Fr = Infinity)
Wio (Fr = 10)
Wio (Fr = 5)
Wio (Fr = 2)
Wio (Fr = 1.58)
Wio (Fr = 1.015)
Wio (Fr = 1)
Wio (Fr = 0.75)
Wio (Fr = 0.5)

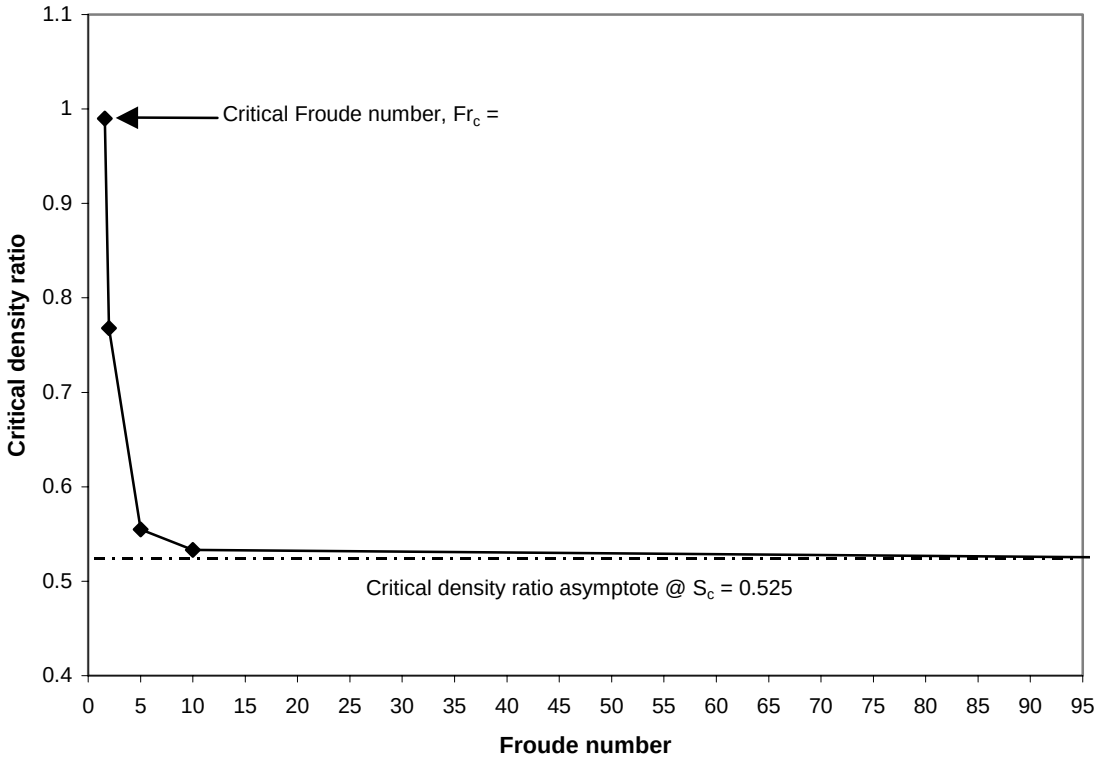
1.1
1
0.9
0.8
0.7
0.6
0.5
0.4
Critical density ratio
Critical Froude number, Fr$_c$ =
Critical density ratio asymptote @ S$_c$ = 0.525
0
5
10
15
20
25
30
35
40
45
50
55
60
65
70
75
80
85
90
95
Froude number

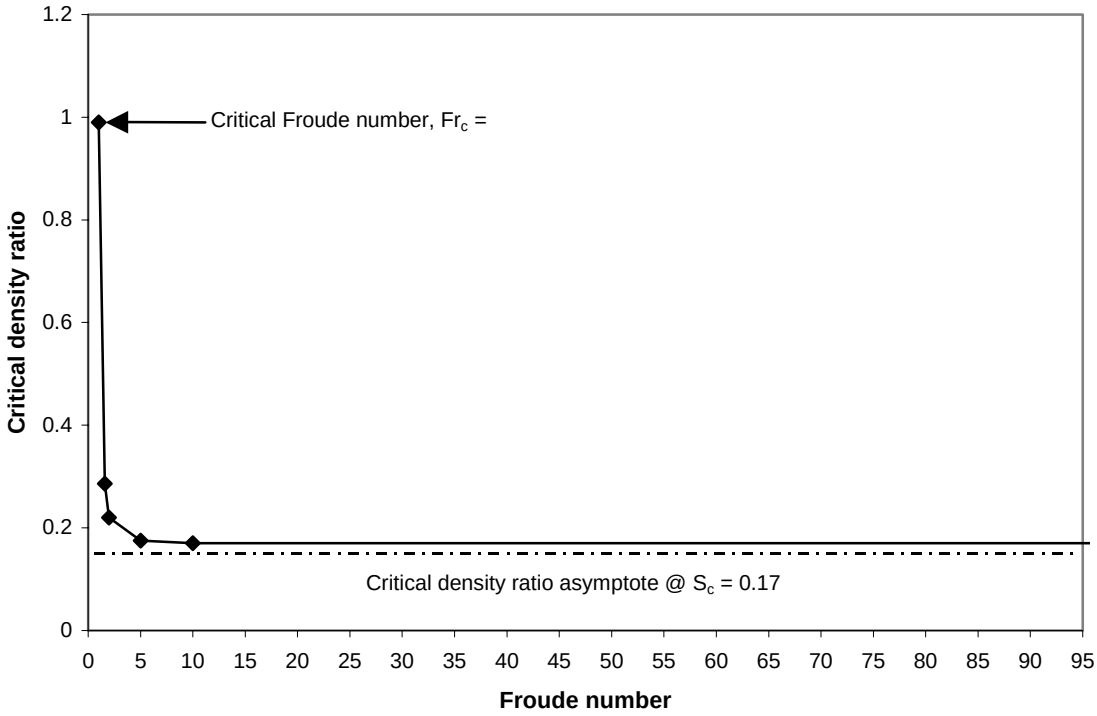
1.2
1
0.8
0.6
0.4
0.2
0
Critical density ratio
Critical Froude number, Fr$_c$ =
Critical density ratio asymptote @ S$_c$ = 0.17
0 5 10 15 20 25 30 35 40 45 50 55 60 65 70 75 80 85 90 95
Froude number

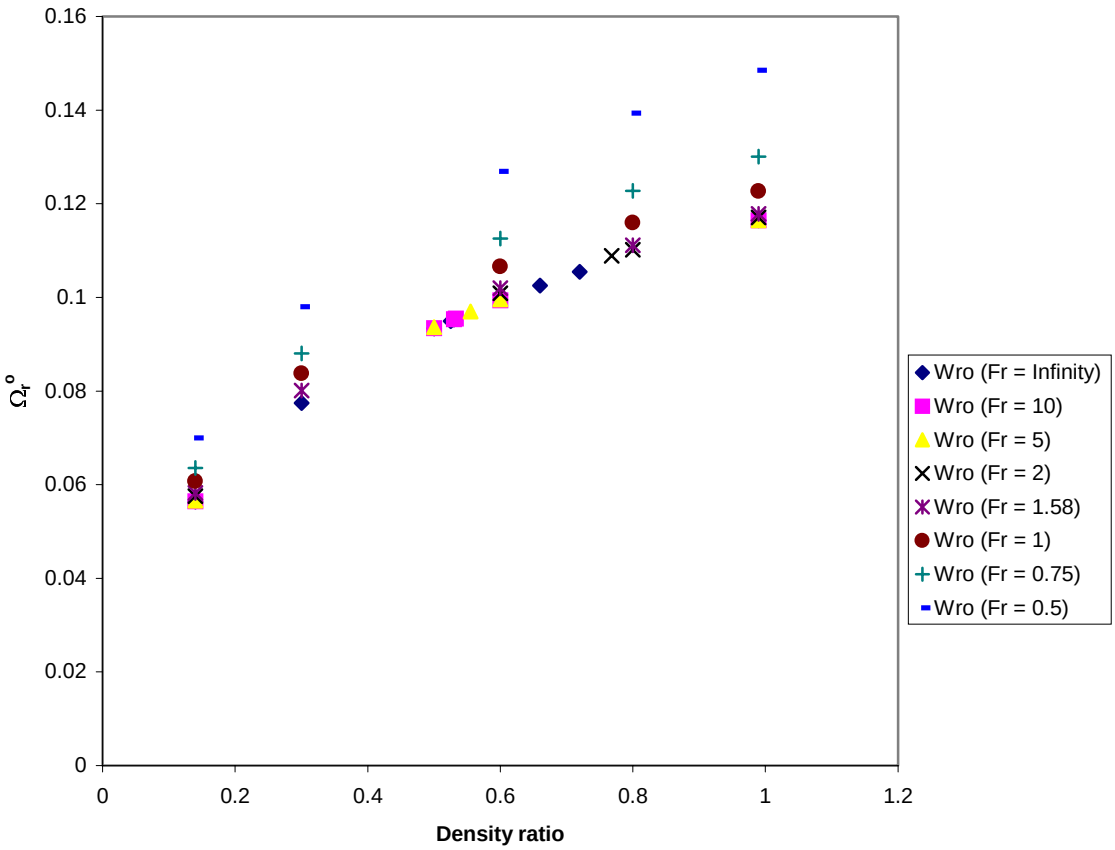
0.16
0.14
0.12
0.1
0.08
0.06
0.04
0.02
0
Ω_r^o
0
0.2
0.4
0.6
0.8
1
1.2
Density ratio
Wro (Fr = Infinity)
Wro (Fr = 10)
Wro (Fr = 5)
Wro (Fr = 2)
Wro (Fr = 1.58)
Wro (Fr = 1)
Wro (Fr = 0.75)
Wro (Fr = 0.5)

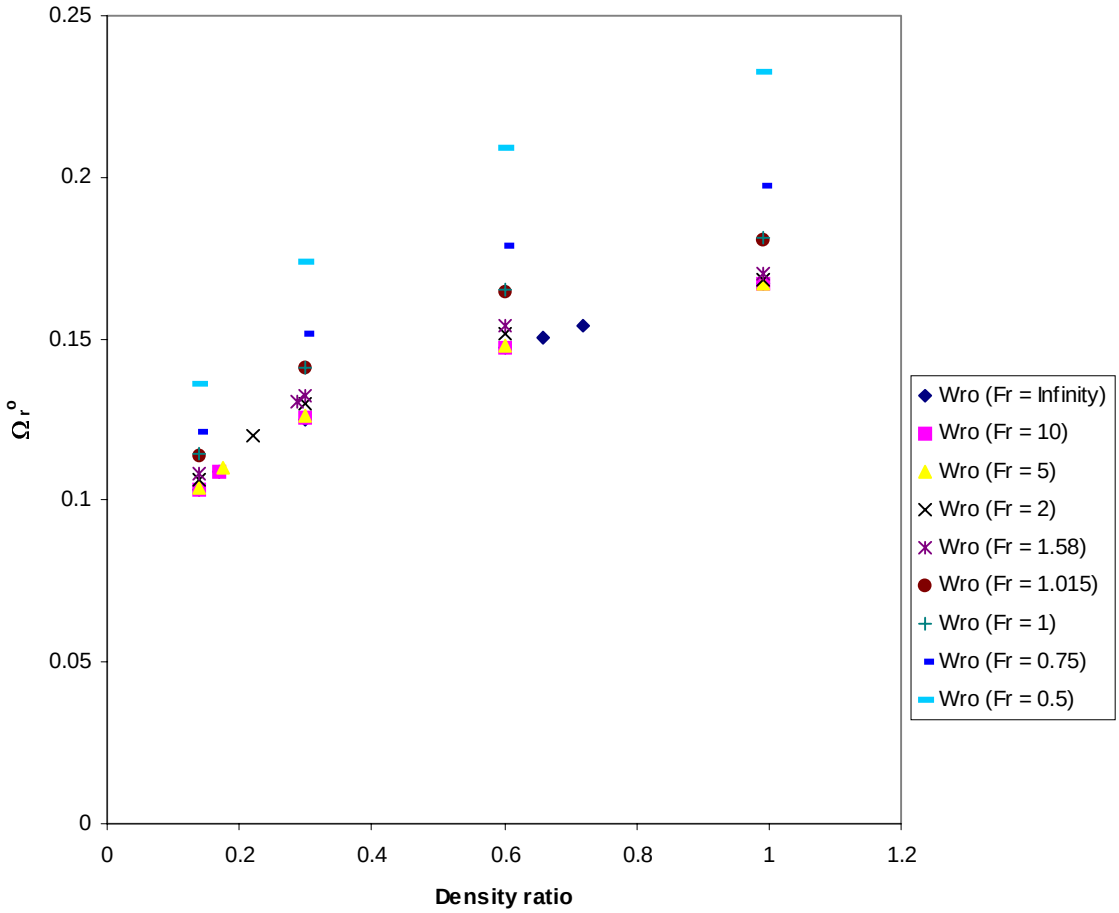
0.25
0.2
0.15
0.1
0.05
0
Ω r°
0
0.2
0.4
0.6
0.8
1
1.2
Density ratio
Wro (Fr = Infinity)
Wro (Fr = 10)
Wro (Fr = 5)
Wro (Fr = 2)
Wro (Fr = 1.58)
Wro (Fr = 1.015)
Wro (Fr = 1)
Wro (Fr = 0.75)
Wro (Fr = 0.5)

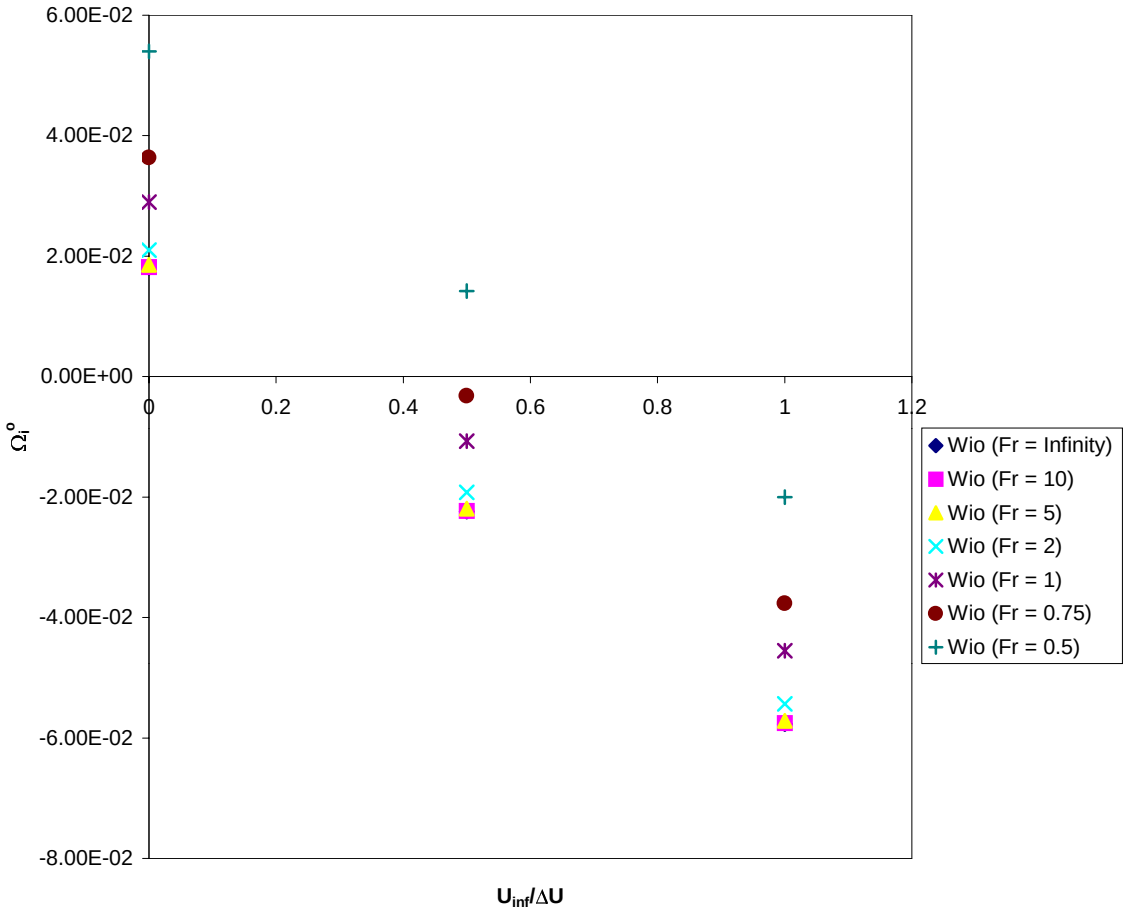
6.00E-02
4.00E-02
2.00E-02
0.00E+00
-2.00E-02
-4.00E-02
-6.00E-02
-8.00E-02
0
0.2
0.4
0.6
0.8
1
1.2
Ω°i
U_inf/ΔU
Wio (Fr = Infinity)
Wio (Fr = 10)
Wio (Fr = 5)
Wio (Fr = 2)
Wio (Fr = 1)
Wio (Fr = 0.75)
Wio (Fr = 0.5)

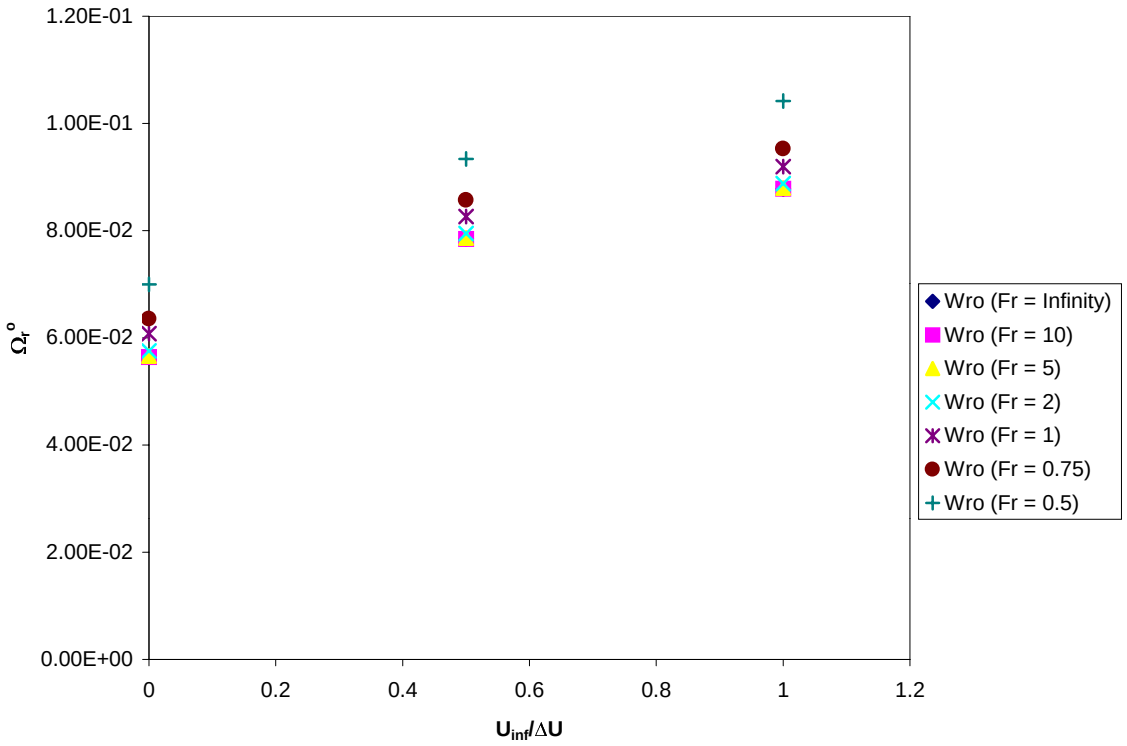
1.20E-01
1.00E-01
8.00E-02
6.00E-02
4.00E-02
2.00E-02
0.00E+00
Ω_r°
0
0.2
0.4
0.6
0.8
1
1.2
$U_{inf}/\Delta U$
Wro (Fr = Infinity)
Wro (Fr = 10)
Wro (Fr = 5)
Wro (Fr = 2)
Wro (Fr = 1)
Wro (Fr = 0.75)
Wro (Fr = 0.5)

Conference Papers (Published)

1. Pasumarthi, K., and Agrawal, A.K., 2004, "Schlieren Measurements of Buoyancy Effects on Flow Transition in Low-Density Gas Jets," ASME Heat Transfer-Fluid Engineering Conference, *ASME HT-FED2004-56810*, July 2004.

2. Satti, R.P., and Agrawal, A.K., 2004, "Numerical Analysis of Flow Evolution in a Helium Jet Injected into Air," ASME Heat Transfer-Fluid Engineering Conference, *ASME HT-FED2004-56811*, July 2004.

3. Vedantam, N. K. and Parthasarathy, R. N. 2004, "Effects of Mean Flow Profiles on the Instability of a Low-Density Gas Jet Injected into a High-Density Gas," ASME Heat Transfer-Fluid Engineering Conference, *ASME HT-FED2004-56794*.

4. Yildrim, B.S., Pasumarthi, K.S., and Agrawal, A.K., 2004, "Concentration Measurements in Self-Excited Momentum-Dominated Low-Density Gas Jets," AIAA Paper-2004-1279.

5. Satti, R., Pasumarthi, K.S., and Agrawal, A.K., 2004, "Numerical Simulations of Buoyancy Effects in Low-Density Gas Jets," AIAA Paper-2004-1317.

6. Yep, Tze-Wing, Agrawal, A.K., and Griffin, D.W., 2002, "Gravitational Effects on Near Field Flow Structure of Low-Density Gas Jets," *AIAA Paper 2002-0761*.

7. Lawson, A. L. and Parthasarathy, R. N. 2002, "Linear Temporal Instability Analysis of a Low-Density Round Gas Jet Injected into a High-Density Gas," *ASME 2002 Energy Technology Conference and Exposition*, ASME Paper ETCE2002/CAE-29010.